J|A|C|S
ARTICLES
Published on Web 05/04/2007

The Sila-Explosives $Si(CH_2N_3)_4$ and $Si(CH_2ONO_2)_4$: Silicon Analogues of the Common Explosives Pentaerythrityl Tetraazide, $C(CH_2N_3)_4$, and Pentaerythritol Tetranitrate, $C(CH_2ONO_2)_4$

Thomas M. Klapötke,*,† Burkhard Krumm,† Rainer Ilg,‡ Dennis Troegel,‡ and Reinhold Tacke*,‡

Contribution from the Department of Chemistry and Biochemistry, Ludwig-Maximilians-University of Munich, Butenandtstrasse 5-13(D), D-81377 Munich, Germany and University of Würzburg, Institute of Inorganic Chemistry, Am Hubland, D-97074 Würzburg, Germany

Received February 27, 2007; E-mail: tmk@cup.uni-muenchen.de; r.tacke@mail.uni-wuerzburg.de

Abstract: The reaction of tetrakis(chloromethyl)silane, $Si(CH_2Cl)_4$, with sodium azide afforded tetrakis(azidomethyl)silane (sila-pentaerythrityl tetraazide, $Si(CH_2N_3)_4$ (**1b**)). Nitration of tetrakis(hydroxymethyl)silane, $Si(CH_2OH)_4$, with nitric acid resulted in the formation of tetrakis(nitratomethyl)silane (sila-pentaerythritol tetranitrate, $Si(CH_2ONO_2)_4$ (**2b**)). Compounds **1b** and **2b** are extremely shock-sensitive materials and very difficult to handle. Spectroscopic data were obtained as good as sensitivity and safety allowed for umambiguous identification. Quantum chemical calculations (DFT) of the C/Si pairs $C(CH_2OH)_4/Si(CH_2OH)_4$, **1a**/**1b**, and **2a**/**2b** regarding the structures and electronic populations were performed.

Introduction

The neopentane derivatives pentaerythrityl tetraazide, $C(CH_2N_3)_4$ (**1a**),[1,2] and pentaerythritol tetranitrate (Nitropenta, PETN), $C(CH_2ONO_2)_4$ (**2a**), are well-known compounds for many years, compound **2a** in particular, and have been studied for their explosive properties.[3−5] Great interest in studying the properties of **2a** is demonstrated by the very recent literature.[6−9] Furthermore, the crystal structure of **1a**[10] has also been reinvestigated very recently.[11] The precursors for these energetic materials, pentaerythrityl tetrachloride/bromide, $C(CH_2X)_4$ (X = Cl, Br), and pentaerythritol, $C(CH_2OH)_4$, are easily available and produced in bulk. Very recently, the synthesis of their silicon analogues $Si(CH_2X)_4$ (X = Cl, Br) and $Si(CH_2OH)_4$ and other derivatives of the formula type $Si(CH_2X)_4$ have been reported.[12,13] It was therefore of interest whether the hitherto unknown sila-analogues of **1a** and **2a**, compounds **1b** and **2b**, are accessible and if their explosive properties are comparable to those of the parent carbon compounds.

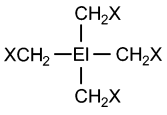

	El	X
1a	C	N_3
1b	Si	N_3
2a	C	ONO_2
2b	Si	ONO_2

Results and Discussion

Treatment of tetrakis(chloromethyl)silane[12] with excess sodium azide in acetone at ambient temperature yielded tetrakis(azidomethyl)silane (sila-pentaerythrityl tetraazide), $Si(CH_2N_3)_4$ (**1b**) (eq 1).

$$Si(CH_2Cl)_4 \xrightarrow{\text{excess } NaN_3/25\ ^\circ C/\text{acetone}} \underset{\mathbf{1b}}{Si(CH_2N_3)_4} \qquad (1)$$

Compound **1b** was isolated as a colorless liquid (no crystallization at ≥ −20 °C), which is very sensitive to shock or friction. In solution, no indication of decomposition was observed. The pure substance was shown to be stable over a period of 1.5 years at ambient temperature by comparison of the Raman spectra (Figure 1), which were almost identical. The

† University of Munich.
‡ University of Würzburg.

(1) Fleischer, E. B.; Gebala, A. E.; Levey, A.; Tasker, P. A. *J. Org. Chem.* **1971**, *36*, 3042−3044.
(2) Hayes, W.; Osborn, H. M. I.; Osborne, S. D.; Rastall, R. A.; Romagnoli, B. *Tetrahedron* **2003**, *59*, 7983−7996.
(3) Dunn, T. J.; Neumann, W. L.; Rogic, M. M.; Woulfe, S. R. *J. Org. Chem.* **1990**, *55*, 6368−6373.
(4) Köhler, J.; Meyer, R. *Explosivstoffe*, 9th ed.; Wiley-VCH: Weinheim, Germany, 1998.
(5) Anderson, W. S.; Hyer, H. J.; Sundberg, J. E.; Rudy, T. P. *Ind. Eng. Chem. Res.* **2000**, *39*, 4011−4013.
(6) Gruzdkov, Y. A.; Gupta, Y. M. *J. Phys. Chem. A* **2000**, *104*, 11169−11176.
(7) Gruzdkov, Y. A.; Gupta, Y. M. *J. Phys. Chem. A* **2001**, *105*, 6197−6202.
(8) Gruzdkov, Y. A.; Dreger, Z. A.; Gupta, Y. M. *J. Phys. Chem. A* **2004**, *108*, 6216−6221.
(9) Zhurova, E. A.; Stash, A. I.; Tsirelson, V. G.; Zhurov, V. V.; Bartashevich, E. V.; Potemkin, V. A.; Pinkerton, A. A. *J. Am. Chem. Soc.* **2006**, *128*, 14728−14734.
(10) Cady, H. H.; Larson, A. C. *Acta. Crystallogr.* **1975**, *B31*, 1864−1869.
(11) Lyssenko, K. A.; Nelubina, Y. V.; Safronov, D. V.; Haustova, O. I.; Kostyanovsky, R. G.; Lenev, D. A.; Antipin, M. Y. *Mendeleev Commun.* **2005**, 232−234.
(12) Daiss, J. O.; Barth, K. A.; Burschka, C.; Hey, P.; Ilg, R.; Klemm, K.; Richter, I.; Wagner, S. A.; Tacke, R. *Organometallics* **2004**, *23*, 5193−5197.
(13) Ilg, R.; Troegel, D.; Burschka, C.; Tacke, R. *Organometallics* **2006**, *25*, 548−551.

10.1021/ja071299p CCC: $37.00

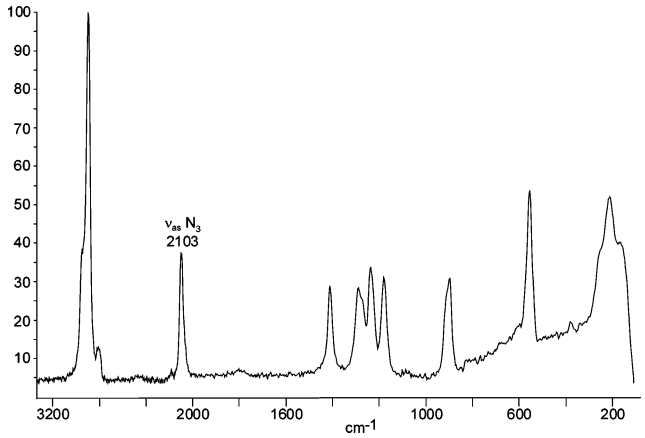

Figure 1. Raman spectrum of $Si(CH_2N_3)_4$ (**1b**) (1084 nm, 100 mW, 25 °C).

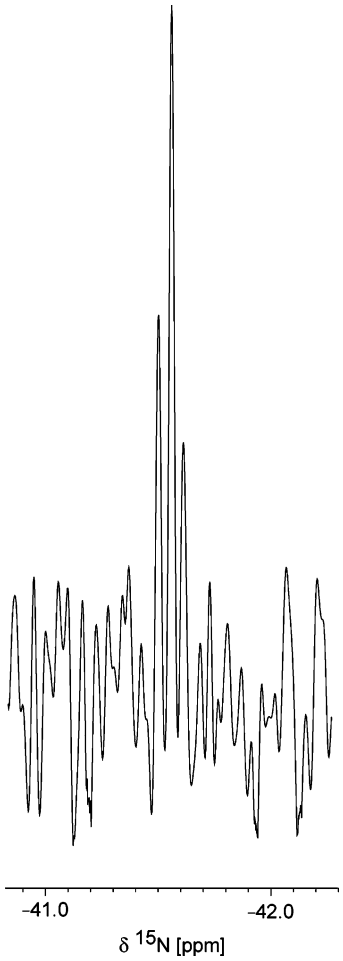

Figure 2. ^{15}N NMR spectrum of $Si(CH_2ONO_2)_4$ (**2b**) in 1,2-$ClCH_2CH_2Cl$ (40.6 MHz, benzene-d_6 lock capillary, 25 °C, natural abundance of ^{15}N).

antisymmetric, azide-stretching vibration is located in the typical region for covalent azides around 2100 cm^{-1}.

The NMR data of compound **1b** clearly support its proposed constitution. The ^{29}Si NMR resonance signal at δ −2.1 ppm is found in a similar region as those of the silanes $Si(CH_2Cl)_4$ (δ −0.7 ppm)[12] and $Si(CH_2Br)_4$ (δ −1.6 ppm).[13] In the ^{15}N NMR spectrum three resonance signals in the typical region for covalent azides are found; the central (β) nitrogen atom shows

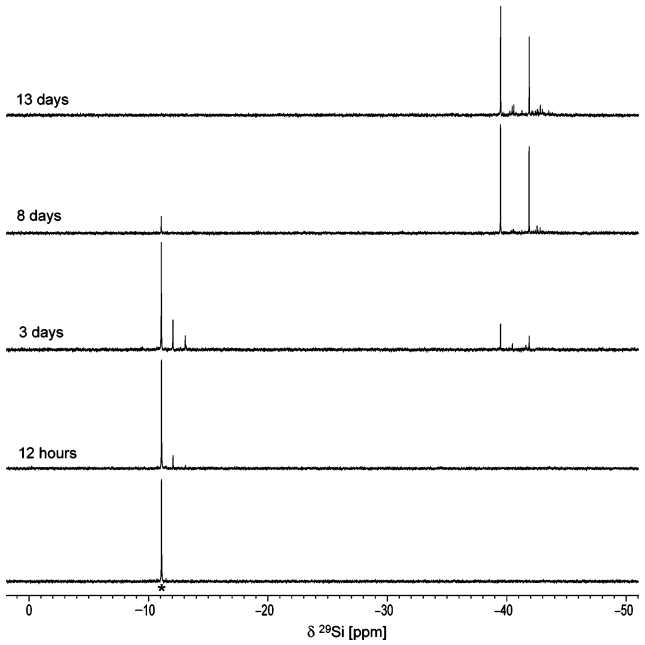

Figure 3. $^{29}Si\{^1H\}$ NMR spectra of $Si(CH_2ONO_2)_4$ (**2b**) in 1,2-dichloroethane as a function of time monitoring the decomposition of **2b** (79.5 MHz, benzene-d_6 lock capillary, 25 °C). The resonance signal for **2b** is marked with an asterisk.

a coupling with the methylene hydrogen atoms ($^3J_{N-H}$ = 6.9 Hz). The typical satellite pattern due to the ^{29}Si nucleus is observed in the ^1H and $^{13}C\{^1H\}$ NMR spectra.

Treatment of tetrakis(hydroxymethyl)silane with excess nitric acid (100%) in 1,2-dichloroethane (DCE) at 0 °C resulted in the formation of pure tetrakis(nitratomethyl)silane (sila-pentaerythritol tetranitrate, Si-PETN), $Si(CH_2ONO_2)_4$ (**2b**) (eq 2). The nitration was carried out similarly to a procedure reported for the nitration of pentaerythritol, employing rather smooth conditions, which in that case led to partial nitrated products (mono- and bis-nitrated).[14] By contrast, nitration of sila-pentaerythritol yielded exclusively the tetranitrated product **2b**.

$$Si(CH_2OH)_4 \xrightarrow{\text{excess } HNO_3/0\ ^\circ C/DCE} \underset{\mathbf{2b}}{Si(CH_2ONO_2)_4} \qquad (2)$$

The silicon compound **2b** is an extremely dangerous material, superior to its derivative **1b**. The crystalline compound exploded on every occasion upon contact with a Teflon spatula. Compound **2b** was characterized only by means of NMR spectroscopy. Because of its extreme sensitivity, no other methods for characterization were possible. On one occasion crystalline material was selected for X-ray diffraction studies and exploded under the microscope. Solutions of **2b** in diethyl ether exploded upon the slightest evaporation of the solvent. Concentrated solutions of **2b** in 1,2-dichloroethane, however, could be handled safely, and all NMR measurements were conducted in this solvent. On the basis of the NMR data obtained, we could unambiguously confirm the formation of **2b** as the sole product. The ^{29}Si NMR resonance signal consists of a nonet due to coupling of the ^{29}Si nucleus with the eight equivalent hydrogen atoms of the four methylene groups. The ^{29}Si NMR resonance

(14) Korolev, A. M.; Eremenko, L. T.; Meshikhina, L. V.; Eremenko, I. L.; Aleksandrov, G. G.; Konovalova, N. P.; Lodygina, V. P. *Russ. Chem. Bull., Int. Ed.* **2003**, *52*, 1859−1863.

Table 1. Calculated Structural Parameters of **1a**, **1b**, **2a**, and **2b** (Geometry Optimization at the B3LYP/6-31G(d) Level)

	$C(CH_2N_3)_4$ **(1a)**	$Si(CH_2N_3)_4$ **(1b)**	$C(CH_2ONO_2)_4$ **(2a)**	$Si(CH_2ONO_2)_4$ **(2b)**
point group	S_4	S_4	S_4	S_4
$-E$/au	852.090122	1103.486303	1316.469107	1567.870031
NIMAG	0	0	0	0
dipole moment/D	0.8	0.8	0.0	0.0
zpe/kcal mol^{-1}	110.2	102.9	119.1	112.2
d(El−C)/Å (El = C, Si)	1.542	1.901	1.544	1.906
d(C−ONO_2)/Å			1.440	1.430
d(C−N_3)/Å	1.483	1.487		
d(N_α−N_β)/Å	1.245	1.237		
d(N_β−N_γ)/Å	1.142	1.142		
d(O−NO_2)/Å			1.430	1.440
d(N−O_{term})/Å			1.210, 1.200	1.200, 1.200
∠(ElCY)/deg (El = C, Si; Y = N, O)	109.1	107.4	106.4	104.4
∠(CElC)/deg (El = C, Si)	109.0, 110.3	109.3, 109.8	108.7, 111.0	109.0, 110.3
∠(NNN)/deg	173.4	173.2		
∠($O_{term}NO_{term}$)/deg			130.7	131.0
∠(CNN)/deg	115.7	115.9		

signal of **2b** located at δ −11.1 ppm is significantly high-field shifted compared to that of its azide derivative **1b** (δ −2.1 ppm), and as expected, the chemical shift is similar to that of the precursor $Si(CH_2OH)_4$ (δ −9.9 ppm).[13] In the ^{1}H and ^{13}C{^{1}H} NMR spectra a typical satellite pattern due to the ^{29}Si nucleus is detected, and low-field shifted resonance signals compared to those of **1b** are observed. The ^{15}N NMR resonance signal consists of a triplet due to coupling of the ^{15}N nucleus with the two hydrogen atoms of the methylene group ($^3J_{N-H}$ = 4.3 Hz), therefore confirming the presence of the CH_2ONO_2 unit (Figure 2).

After 12 h, a significant degree of decomposition of **2b** was observed by ^{29}Si NMR spectroscopy. Therefore, a study of the progressive decomposition was performed by measuring the ^{29}Si NMR spectra of a solution of **2b** in 1,2-dichloroethane as a function of time (Figure 3). Also based on our experience, it is advisable to avoid neutralization of the original reaction mixture. ^{29}Si NMR studies of alkalized reaction mixtures revealed rapid formation of other silicon-containing products, which are probably due to partially decomposed **2b**. Simple extraction of the organic phase, after dilution of the nitric acid phase with ice, furnished NMR spectroscopically pure **2b** (see also bottom spectrum, Figure 3).

The proton-coupled ^{29}Si NMR spectrum of **2b** shows after 8 days two quintets for the resonances at −39.5 and −41.9 ppm, which indicates two methylene groups bound to silicon. The region around −40 ppm is typical for aliphatic difunctional siloxanes.[15] Based on the ^{29}Si NMR results the decomposition products of **2b** must contain a siloxane feature of the type −OSi-$(CH_2OR)_2$O−. Whether there are still nitro groups, denoted as R attached to the CH_2O moieties, cannot be definitely confirmed, since the ^{14}N NMR spectrum showed only minor amounts of nitrato groups. In addition, dinitrogen (−72 ppm) and nitrito groups (−CH_2ONO, characteristic region around +185 ppm) were present after few days.

Theoretical Studies

In an effort to find out why $Si(CH_2ONO_2)_4$ (**2b**) has such a drastically increased sensitivity compared to its carbon analogue $C(CH_2ONO_2)_4$ (**2a**), and also because of the lack of structural data, extensive calculations were performed. The impact sensitivity of **2a** is reported to be 3 Nm,[4] whereas its silicon analogue **2b** is even more sensitive with an impact sensitivity of <1 Nm (BAM drophammer test).

DFT Calculations. The molecular structures and vibrational frequencies of $C(CH_2N_3)_4$ (**1a**), $Si(CH_2N_3)_4$ (**1b**), $C(CH_2ONO_2)_4$ (**2a**), and $Si(CH_2ONO_2)_4$ (**2b**) were calculated and optimized at the hybrid density functional B3LYP level of theory using a polarized double-ζ 6-31G(d) basis set for all elements. Table 1 summarizes the structural computational results, Table 2 contains characteristic (high intensity) IR and Raman vibrations. As can be seen from Table 3, the agreement between the computed, scaled, and experimentally observed Raman frequencies for the new silicon compound **1b** is very good. Figure 4 shows the optimized molecular structures of the silicon compounds **1b** and **2b**. The calculated structure of **1a** is in good agreement with the earlier work.[11]

Electrostatic Potential. The electrostatic potentials of **1a**, **1b**, **2a**, **2b**, $C(CH_2OH)_4$, and $Si(CH_2OH)_4$ were computed at optimized structures at the B3LYP/6-31G(d) level of theory using the program package HyperChem 7.0.[16] Figures 5−7 illustrate the electrostatic potentials (ESPs) for the 0.001 electron/b^3 (b = bohr) isosurface of electron density evaluated at the B3LYP level of theory. In these figures, the colors range from −0.01 to +0.01 hartree with green denoting extremely electron-deficient regions ($V(r)$ > 0.01 hartree) and red denoting electron-rich regions ($V(r)$ < −0.01 hartree). It has recently been found by Politzer et al.[17−20] and extensively used and further developed by Rice et al.[21−24] that the patterns of the computed electrostatic potential (see eq 3) on the surface of molecules in general can be related to the sensitivity of the bulk material. While in nitro and azido systems the regions of positive potential are almost universally more extensive in area, in the subset they are also

(15) Williams, E. A. Recent Advances in Silicon-29 NMR Spectroscopy. In *Annu. Rep. NMR Spectrosc*; Webb, G. A., Ed.; Academic Press: London (UK), 1983; Vol. 15, pp 235−282.

(16) *HyperChem 7.0*, Molecular Visualization and Simulation Program Package, Hypercube: Gainesville, FL, 2002.
(17) Murray, J. S.; Lane, P.; Politzer, P. *Mol. Phys.* **1995**, *85*, 1−8.
(18) Murray, J. S.; Lane, P.; Politzer, P. *Mol. Phys.* **1998**, *93*, 187−194.
(19) Politzer, P.; Murray, J. S. Computational Characterization of Energetic Materials. In *Pauling's Legacy: Modern Modelling of the Chemical Bond*; Maksic, Z. B., Orville-Thomas, W. J., Eds.; Theoretical and Computational Chemistry, Vol. 6; Elsevier: New York, 1999; pp 347−363.
(20) Politzer, P.; Murray, J. S.; Seminario, J. M.; Lane, P.; Grice, M. E.; Concha, M. C. *J. Mol. Struct. (THEOCHEM)* **2001**, *573*, 1−10.
(21) Rice, B. M.; Chabalowski, C. F.; Adams, G. F.; Mowrey, R. C.; Page, M. *Chem. Phys. Lett.* **1991**, *184*, 335−342.
(22) Rice, B. M.; Hare, J. J. *J. Phys. Chem. A* **2002**, *106*, 1770−1783.
(23) Rice, B. M.; Sahu, S.; Owens, F. J. *J. Mol. Struct. (THEOCHEM.)* **2002**, *583*, 69−72.
(24) Rice, B. M. *Adv. Ser. Phys. Chem.* **2005**, *16*, 335−367.

Table 2. Computed IR and Raman Frequencies of **1a**, **1b**, **2a**, and **2b** at the B3LYP/6-31G(d) Level[a]

	$C(CH_2N_3)_4$ **(1a)**	$Si(CH_2N_3)_4$ **(1b)**		$C(CH_2ONO_2)_4$ **(2a)**	$Si(CH_2ONO_2)_4$ **(2b)**
			IR		
$\delta(N_3)$	654 (2)	606 (3)	υ(Si−C)		642 (18)
$\rho(CH_2)$	916 (2)	854 (9)	υ(O−NO_2)	709 (6)	644 (31)
$\rho(CH_2)$	1285 (1)	1214 (12)	$\omega(NO_3)$	759 (8)	749 (15)
		1282 (12)	υ(O−NO_2)	855 (50)	827 (59)
		1290 (25)	υ(O−NO_2)	860 (100)	831 (100)
$\upsilon_{sym}(N_3)$	1346 (16)	1322 (9)	υ(C−ONO_2)	1037 (10)	1027 (2)
$\upsilon_{sym}(N_3)$	1348 (35)	1323 (19)	υ(C−ONO_2)	1075 (16)	1036 (4)
$\delta(CH_2)$	1518 (1)	1488 (5)	δ(C−H)	1317 (35)	1288 (7)
$\delta(CH_2)$	1524 (4)	1489 (4)			1294 (6)
$\upsilon_{as}(N_3)$	2267 (54)	2256 (51)	δ(C−H)	1336 (38)	1363 (59)
$\upsilon_{as}(N_3)$	2268 (100)	2258 (100)	δ(C−H)	1350 (30)	1365 (96)
			$\upsilon(NO_2)$	1776 (28)	1782 (24)
			$\upsilon(NO_2)$	1777 (72)	1783 (100)
	$C(CH_2N_3)_4$ **(1a)**	$Si(CH_2N_3)_4$ **(1b)**		$C(CH_2ONO_2)_4$ **(2a)**	$Si(CH_2ONO_2)_4$ **(2b)**
			Raman		
υ(C−N_3)		927 (7)	υ(O−NO_2)	885 (28)	849 (39)
υ(C−N_3)	954 (6)	937 (3)	δ(C−H)	1270 (10)	1229 (7)
$\rho(CH_2)$	1264 (10)	1286 (6)	δ(C−H)	1434 (4)	1375 (6)
$\upsilon_{sym}(N_3)$	1350 (10)	1325 (10)	δ(C−H)	1536 (7)	1511 (10)
$\delta(CH_2)$	1518 (8)	1488 (10)	υ(C−H)	3106 (100)	3065 (100)
$\upsilon_{as}(N_3)$	2267 (12)	2256 (12)	υ(C−H)	3160 (14)	3118 (21)
$\upsilon_{as}(N_3)$	2268 (5)	2258 (6)	υ(C−H)	3163 (19)	3119 (29)
$\upsilon_{as}(N_3)$	2282 (19)	2268 (21)			
υ_{sym}(C−H)	3057 (100)	3026 (100)			
υ_{as}(C−H)	3102 (15)	3072 (21)			
υ_{as}(C−H)	3104 (13)	3073 (23)			

[a] Relative intensity (strongest peak = 100) in parentheses.

Table 3. Computed (B3LYP/6-31G(d) Level), Scaled (0.96), and Experimentally Observed Raman Frequencies for $Si(CH_2N_3)_4$ (**1b**)[a]

vibration	B3LYP/6-31G(d)	scaled (0.96)	observed
υ(C−N_3)	927 (7)	890	899 (30)
υ(C−N_3)	937 (3)	900	900 (sh)
$\rho(CH_2)$	1286 (6)	1235	1238 (33)
$\upsilon_{sym}(N_3)$	1325 (10)	1272	1291 (28)
$\delta(CH_2)$	1488 (10)	1428	1412 (29)
$\upsilon_{as}(N_3)$	2256 (12)	2166	2096 (37)
$\upsilon_{as}(N_3)$	2258 (6)	2168	
$\upsilon_{as}(N_3)$	2268 (21)	2177	2103 (37)
υ_{sym}(C−H)	3026 (100)	2904	2897 (100)
υ_{as}(C−H)	3072 (21)	2949	
υ_{as}(C−H)	3073 (23)	2950	2954 (38)

[a] Relative intensity (strongest peak = 100) in parentheses.

Table 4. NAO and NLMO/NPA Bond Orders

		NAO	NLMO/NPA
$C(CH_2N_3)_4$ (**1a**)	C−C	0.83	0.97
	C−N_3	0.79	0.78
	N_α−N_β	1.19	1.21
$Si(CH_2N_3)_4$ **(1b)**	Si−C	0.71	0.51
	C−N_3	0.77	0.80
	N_α−N_β	1.18	1.20
$C(CH_2ONO_2)_4$ (**2a**)	C−C	0.83	0.95
	O−NO_2	0.68	0.84
$Si(CH_2ONO_2)_4$ (**2b**)	Si−C	0.71	0.53
	O−NO_2	0.65	0.82
$C(CH_2OH)_4$	C−C	0.83	0.96
	C−O	0.72	0.67
$Si(CH_2OH)_4$	Si−C	0.71	0.55
	C−O	0.68	0.70

stronger than the negative, contrary to the usual situation. This atypical imbalance between stronger positive regions and weaker negative ones can be related to the impact sensitivities. The electrostatic potential at any point r is given by eq 3 in which Z_A is the charge on nucleus A, located at R_A.

$$V(r) = \sum \{Z_A/(|R_A - r|)\} - \int (\rho(r')\,dr')/(|r' - r|) \quad (3)$$

The relative strengths and size of the regions of positive and negative electrostatic potential on the surfaces of energetic molecules are of great importance. Typically, for organic molecules in general, the negative regions cover a smaller portion of the total surface area but are significantly stronger (in terms of average magnitudes) than the positive ones (see Figure 7 for $C(CH_2OH)_4$ and $Si(CH_2OH)_4$). In the case of energetic molecules, on the other hand, the positive regions are still larger but now also stronger than the negative ones (Figures 5 and 6). Politzer et al. were able to show[17−20] that impact sensitivity can be expressed as a function of the extent of this anomalous reversal of the strengths of the positive and negative surface potentials (Figures 5 and 6). Comparing **2a** with the more sensitive silicon analogue **2b**, the most obvious feature of the ESPs in Figure 6 appears to be the region over the center of the molecule and the extent of the positive potential. For **2a** and **2b** it is interesting to note that the region of electron deficiency is in the middle of the molecule, right around the central C−C and Si−C bonds (Figure 6), and not over the O−NO_2 bonds as one might have expected. This finding is in good accord with a recent atoms in molecules (AIM) study on **2a**,[9] according to which the O−NO_2 bond is relatively strong and probably stronger than the C−C and C−O bonds, which were shown to be first to break when the crystal was exposed to a high-energy laser, high-energy fracture, or high pressure.[6,25,26] (N.B. In contrast, it has been demonstrated that the

(25) Ng, W. L.; Field, J. E.; Hauser, H. M. *J. Appl. Phys.* **1986**, *59*, 3945−3952.

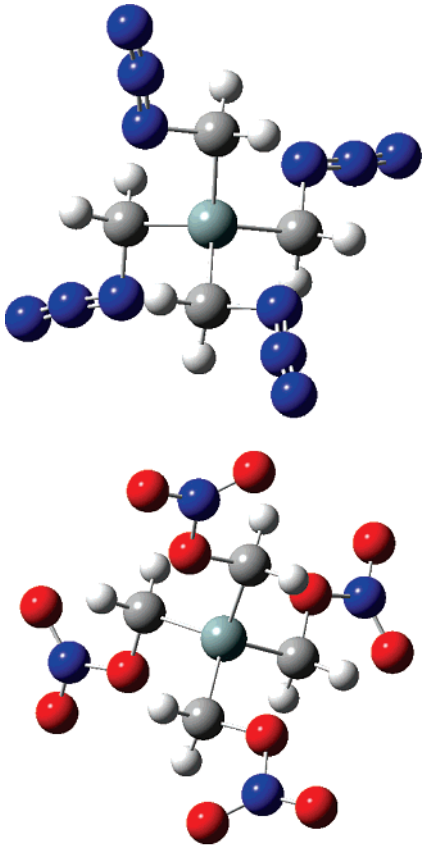

Figure 4. Computed (point group S_4) structures for $Si(CH_2N_3)_4$ (**1b**) (top) and $Si(CH_2ONO_2)_4$ (**2b**) (bottom).

$O-NO_2$ bonds break as the initial step in cases of slow thermal decomposition or exposure to low-energy fracture or low-energy laser at ambient pressures[25,27] with a dissociation energy of 164.2 kJ mol^{-1}).[28] Molecules that are more sensitive to impact have larger electron deficiency in this region than molecules that are less sensitive. Additionally, it seems that the less the electron density is distributed over the body of the molecule (excluding extrema of charge localized over atoms of the electron-donating or electron-withdrawing substituents) the more sensitive the molecule. This effect is also demonstrated in the pairs **1a**/**1b** (Figure 5) and **2a** (sensitive)/**2b** (very shock sensitive) (Figure 6).

The unexpected finding that the impact sensitivity of the silicon compound **2b** is definitely much higher than the sensitivity of its carbon analogue **2a** may be explained by different intermolecular interactions in the condensed phase. In order to elucidate this situation (and since there are no structural X-ray data available for Si−PETN), we carried out further DFT calculations on ensembles of three PETN and three Si−PETN molecules. Three molecules were included in each of the calculations in order to enable the (C or Si central atom) of the central molecule to expand its coordination sphere from four to higher. The structures of both sets of three neutral molecules were fully optimized without symmetry constraints and are shown in Figure 8. Whereas in **2a** the central carbon atom remains tetracoordinate and therefore only bound to four other

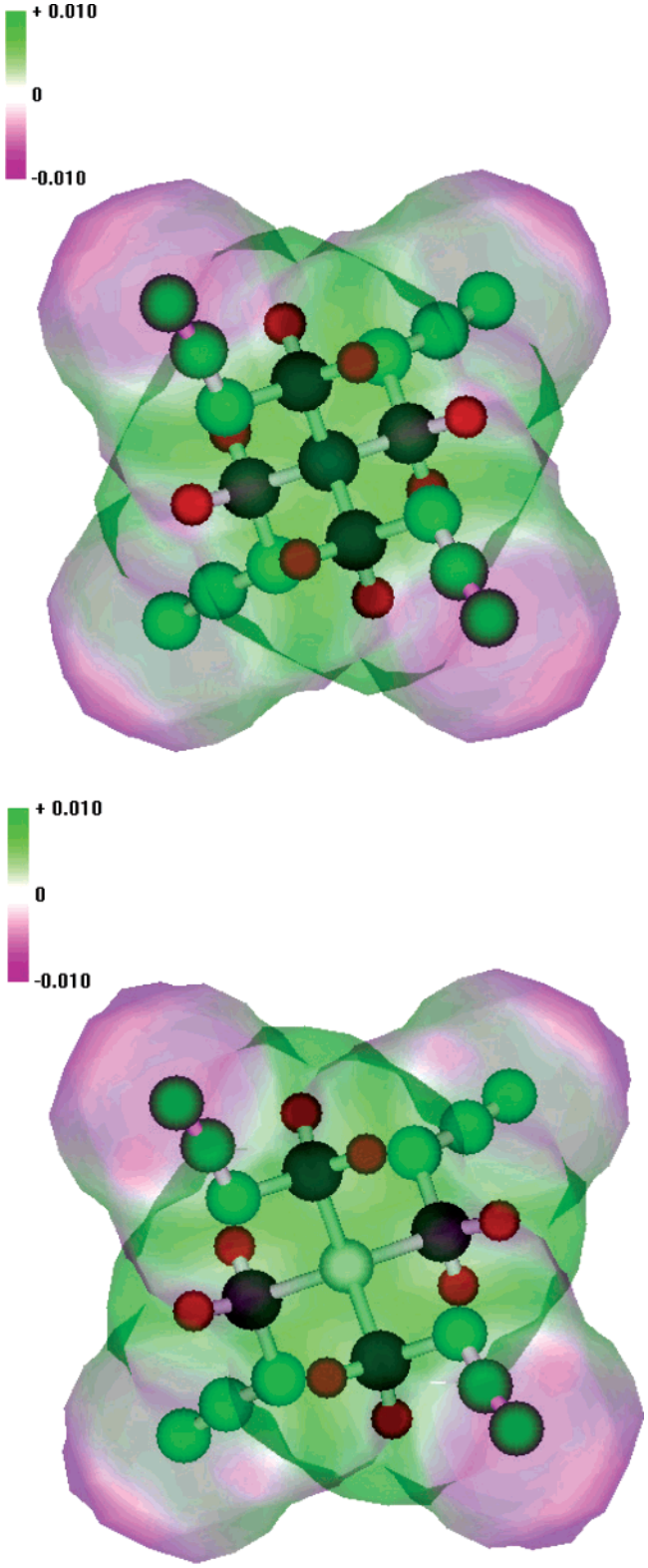

Figure 5. Electrostatic potentials (ESPs) for the 0.001 electron/b^3 isosurface calculated for $C(CH_2N_3)_4$ (**1a**) (top) and $Si(CH_2N_3)_4$ (**1b**) (bottom). Legends for the color ranges of the ESPs are each given in the top left corner and range from −0.01 to +0.01 hartree (au).

carbon atoms, in the silicon analogue **2b** the central silicon atom expands its coordination sphere and shows, in addition to the four Si−C bonds, contacts to four (two chelating) oxygen atoms from neighboring nitrato groups (Figure 8). Figure 8 shows the computed (B3LYP/6-31G(d) level) electrostatic potentials su-

(26) Naud, D. L.; Brower, K. R. *J. Org. Chem.* **1992**, *57*, 3303−3308.
(27) Hiskey, M. A.; Brower, K. R.; Oxley, J. C. *J. Phys. Chem.* **1991**, *95*, 3955−3960.
(28) Khrapkovskii, G. M.; Shamsutdinov, T. F.; Chachkov, D. V.; Shamov, A. G. *J. Mol. Struct. (THEOCHEM)* **2004**, *686*, 185−192.

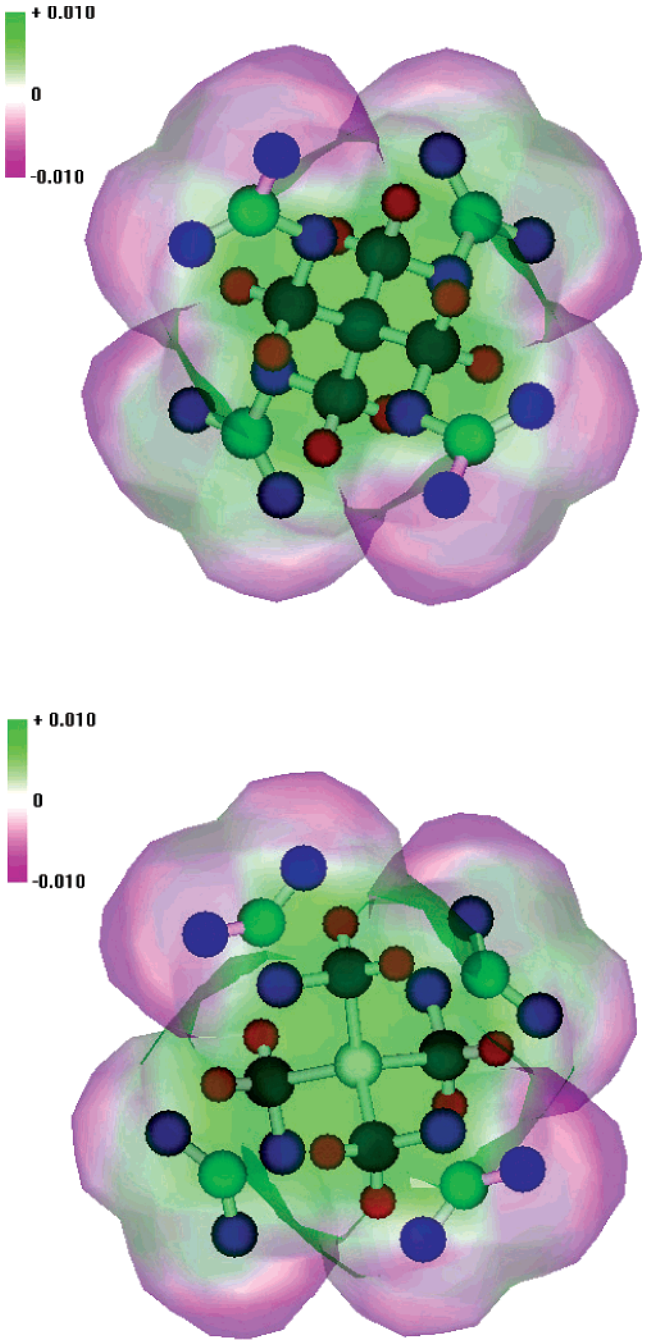

Figure 6. Electrostatic potentials (ESPs) for the 0.001 electron/b^3 isosurface calculated for $C(CH_2ONO_2)_4$ (**2a**) (top) and $Si(CH_2ONO_2)_4$ (**2b**) (bottom). Legends for the color ranges of the ESPs are each given in the top left corner and range from −0.01 to +0.01 hartree (au).

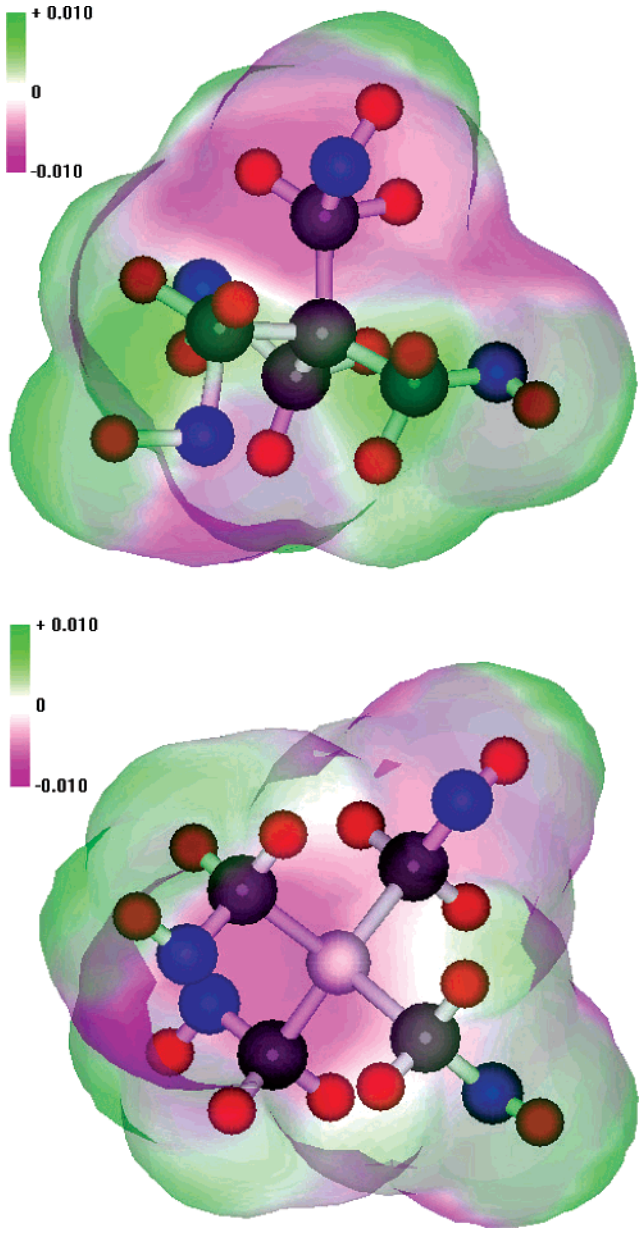

Figure 7. Electrostatic potentials (ESPs) for the 0.001 electron/b^3 isosurface calculated for $C(CH_2OH)_4$ (top) and $Si(CH_2OH)_4$ (bottom). Legends for the color ranges of the ESPs are each given in the top left corner and range from −0.01 to +0.01 hartree (au).

perimposed onto the fully optimized structures for a unit of three PETN (**2a**) (top) and Si−PETN (**2b**) (bottom) molecules. Whereas **2a** shows very long intermolecular C···O−NO_2 distances of >5.0 Å, the average Si···O−NO_2 distances of **2b** are about 4.5 Å. Therefore, exothermic (explosive) decomposition yielding CO_2 (for **2a**) and SiO_2 (for **2b**) may be much more favorable in the latter system. Moreover, the electrostatic potential of **2a** reveals essentially three individual molecules, whereas for the silicon analogue **2b** one system with large (in area and amplitude) positive regions is present.

Population Analyses. For the C/Si analogues **1a**/**1b**, **2a**/**2b**, and $C(CH_2OH)_4$/$Si(CH_2OH)_4$ for comparison a natural bond orbital (NBO) analysis was performed at the B3LYP/6-31G(d) electron density.[29] The NAO and NLMO/NPA bond orders are summarized in Table 4.

As can be seen, the O−NO_2 bonds in the carbon compound **2a** are stronger (bond order, Table 4) and shorter (bond distance, Table 1) than the O−NO_2 bonds in the silicon analogue **2b**. For **2a** and **2b** it is interesting to note that the region of electron deficiency is in the center of the molecule, right around the central C−C and Si−C bonds (Figure 6), and not over the O−NO_2 bonds, as one might have expected. Therefore, the much lower Si−C bond orders in **2b** compared to the C−C bond orders in **2a** (Table 4) may explain the increased sensitivity

(29) Weinhold, F. Natural Bond Orbital Methods. In *Encyclopedia of Computational Chemistry*; Schleyer, P. v. R., Ed.; Wiley: Chichester (UK), 1998; Vol. 3.

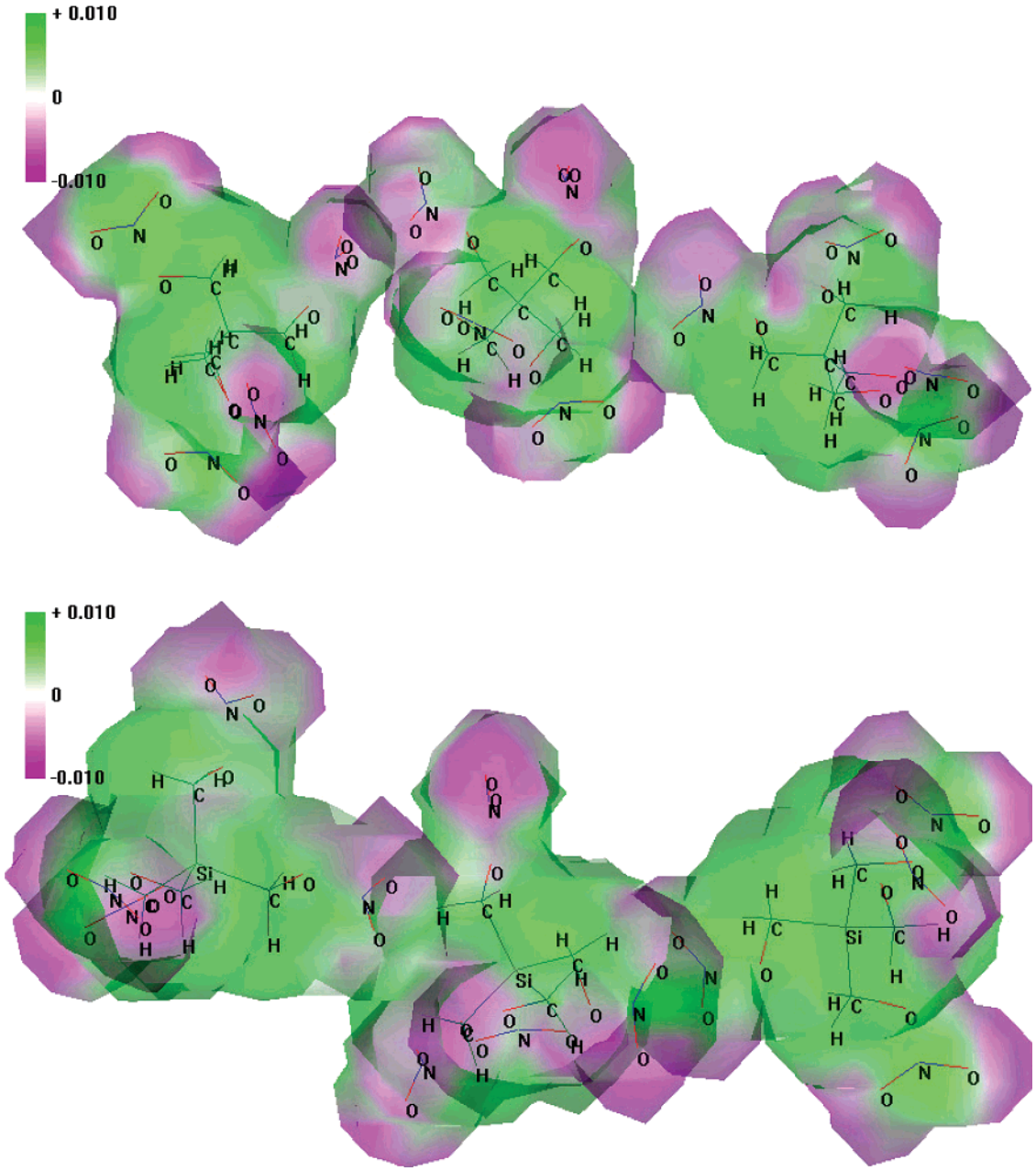

Figure 8. Electrostatic potentials (ESPs) for the 0.001 electron/b^3 isosurface calculated for $[C(CH_2ONO_2)_4]_3$ (top) and $[Si(CH_2ONO_2)_4]_3$ (bottom). Legends for the color ranges of the ESPs are each given in the top left corner and range from −0.01 to +0.01 hartree (au).

of the silicon compound **2b** compared with that of its carbon analogue **2a**.

The same tendency accounts for the azide compounds **1a** and **1b**, with the silicon analogue **1b** showing much higher sensitivity compared to the carbon analogue **1a**.

Experimental Section

Sodium azide and nitric acid (100%, fuming) (Aldrich) were used as received. Tetrakis(chloromethyl)silane, $Si(CH_2Cl)_4$, and tetrakis-(hydroxymethyl)silane, $Si(CH_2OH)_4$, were prepared according to the literature.[12,13] Raman spectra were recorded on a Perkin-Elmer 2000 NIR FT spectrometer fitted with a Nd:YAG laser (1064 nm). NMR spectra were recorded on a JEOL Eclipse 400 instrument at 25 °C, and chemical shifts were determined with respect to $(CH_3)_4Si$ (^{1}H, 399.8 MHz; ^{13}C, 100.5 MHz; ^{29}Si, 79.5 MHz) and CH_3NO_2 (^{14}N, 28.9 MHz; ^{15}N, 40.6 MHz).

CAUTION: All manipulations were performed behind an additional safety shield in a standard, well-ventilated hood. In addition, the experimentalist (B.K.) was always well protected with leather jacket, face shield, and Kevlar gloves.

Tetrakis(azidomethyl)silane, $Si(CH_2N_3)_4$ (1b). A large excess of sodium azide (1.80 g, 27.7 mmol) was added to a solution of tetrakis-(chloromethyl)silane (350 mg, 1.55 mmol) in acetone (5 mL). The mixture was stirred for 2.5 days at 25 °C. The sodium salts were separated from the solution, washed with small amounts of acetone, and then discarded. The reaction solution and wash solution were combined, and the solvent was carefully removed by evaporation to give **1b** in 61% yield (240 mg) as a colorless liquid. ***CAUTION***: Compound **1b** is extremely shock sensitive and explodes upon contact with metal spatula! NMR ($CDCl_3$): ^{1}H, δ 3.15 (CH_2, $^2J_{H-29Si}$ = 5.1 Hz); ^{13}C{^{1}H}, δ 35.3 (CH_2, $^1J_{C-29Si}$ = 58.8 Hz); ^{29}Si{^{1}H}, δ −2.1; ^{15}N, δ −131.7 (N_β, t, $^3J_{N-H}$ = 6.9 Hz), −169.3 (N_γ), −322.8 (N_α).

Raman (100 mW): 2954 (38), 2897 (100), 2810 (13), 2103/2096 (37, $\upsilon_{as}N_3$), 1412 (29), 1291 (28), 1275 (25), 1238 (33), 1180 (31), 899 (30), 557 (53), 381 (19), 255 (37), 211 (52), 169 (40) cm^{-1}.

Tetrakis(nitratomethyl)silane, $Si(CH_2ONO_2)_4$ (2b). Tetrakis(hydroxymethyl)silane (80 mg, 0.52 mmol) was added in one portion at 0 °C to a mixture consisting of 1,2-dichloroethane (3 mL) and nitric acid (100%) (1 mL) in a plastic vessel. The mixture was magnetically stirred for 2 h at 0 °C and then diluted with ice water (3 mL). The organic phase (colorless) was transferred with ***EXTREME CAUTION*** and under full protection with a plastic pipet into an NMR tube. According to the ^{29}Si NMR spectrum, the conversion of tetrakis(hydroxymethyl)-silane into **2b** was quantitative without byproducts. NMR ($ClCH_2CH_2Cl/C_6D_6$ capillary): ^1H, δ 4.42 (CH_2, $^2J_{H-29Si} = 4.5$ Hz); $^{13}C\{^1H\}$, δ 58.9 (CH_2, $^1J_{C-29Si} = 59.2$ Hz); ^{29}Si, δ −11.1 (nonet, $^2J_{Si-H} = 4.7$ Hz); ^{15}N, δ −41.6 (t, $^3J_{N-H} = 4.3$ Hz).

Computational Details. All calculations were carried out using the program package G03W.[30] The structure and frequency calculations were performed with Becke's B3 three-parameter hybrid functional using the LYP correlation functional (B3LYP).[31] For all atoms a standard polarized double-ζ basis set was used (6-31G(d)).[32−36]

Conclusion

In this study, the new silicon analogues of pentaerythrityl tetraazide ($C(CH_2N_3)_4$, **1a**) and pentaerythritol tetranitrate ($C(CH_2ONO_2)_4$, **2a**), compounds $Si(CH_2N_3)_4$ (**1b**) and $Si(CH_2ONO_2)_4$ (**2b**), have been synthesized. The unexpected extreme sensitivity allowed only a characterization by NMR spectroscopy, and in the case of **1b** additionally the Raman spectrum could be recorded. Whereas the liquid silane **1b** is stable at ambient temperature for more than 1 year without noticeable signs of decomposition, the solid silane **2b** decomposes in solution within hours, and is, in neat form, one of the most dangerous materials and tends to explode on the slightest impact. The decomposition of **2b** was monitored by ^{29}Si NMR spectroscopy. On the basis of the superior sensitivity of both **1b** and (even more) **2b**, compared to that of the respective carbon analogues **1a** and **2a**, detailed calculations have been performed. From electrostatic potential and population analysis studies, it can be concluded that the dramatically increased sensitivity of **2b** is likely due to the greater tendency to form Si−O bonds, compared to the formation of C−O bonds in case of **2a**. To the best of our knowledge, this is the first systematic study dealing with sila-explosives.

Acknowledgment. This paper is dedicated to Professor Hans Bürger on occasion of his 70th birthday. We gratefully acknowledge financial support from the University of Munich (LMU), the University of Würzburg, the Fonds der Chemischen Industrie, and the European Research Office (ERO) of the U.S. Army Research Laboratory (ARL) under Contract no. N 62558-05-C-0027.

Supporting Information Available: Complete ref 30. This material is available free of charge via the Internet at http://pubs.acs.org

JA071299P

(30) Frisch, M. J.; et al. *Gaussian 03*; Gaussian Inc.: Pittsburgh PA, 2003.
(31) Miehlich, B.; Savin, A.; Stoll, H.; Preuss, H. *Chem. Phys. Lett.* **1989**, *157*, 200−206.
(32) Ditchfield, R.; Hehre, W. J.; Pople, J. A. *J. Chem. Phys.* **1971**, *54*, 724−728.
(33) Hehre, W. J.; Ditchfield, R.; Pople, J. A. *J. Chem. Phys.* **1972**, *56*, 2257−2261.
(34) Hariharan, P. C.; Pople, J. A. *Mol. Phys.* **1974**, *27*, 209−214.
(35) Gordon, M. S. *Chem. Phys. Lett.* **1980**, *76*, 163−168.
(36) Hariharan, P. C.; Pople, J. A. *Theor. Chim. Acta* **1973**, *28*, 213−222.